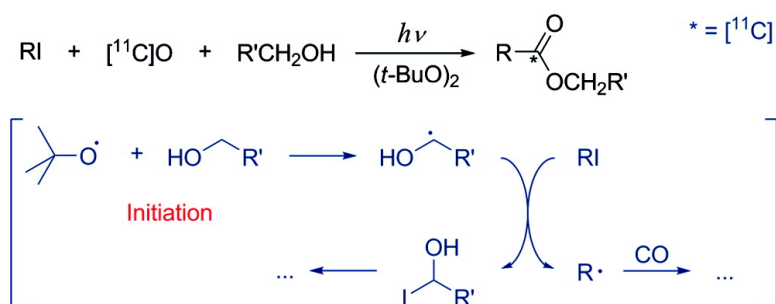**Article**

Radical Carbonylation with [C]Carbon Monoxide Promoted by Oxygen-Centered Radicals: Experimental and DFT Studies of the Mechanism

Oleksiy Itsenko, Daniel Norberg, Torben Rasmussen, Bengt Lngstrm, and Chryssostomos Chatgilialoglu

More About This Article

Additional resources and features associated with this article are available within the HTML version:

- Supporting Information
- Links to the 5 articles that cite this article, as of the time of this article download
- Access to high resolution figures
- Links to articles and content related to this article
- Copyright permission to reproduce figures and/or text from this article

View the Full Text HTML

Radical Carbonylation with [11C]Carbon Monoxide Promoted by Oxygen-Centered Radicals: Experimental and DFT Studies of the Mechanism

Oleksiy Itsenko,*,† Daniel Norberg,# Torben Rasmussen,† Bengt Långström,†,‡ and Chryssostomos Chatgilialoglu*,§

Contribution from the Department of Biochemistry and Organic Chemistry, Uppsala University, Box 576, SE-75123 Uppsala, Sweden, Department of Quantum Chemistry, Uppsala University, Box 518, SE-751 20 Uppsala, Sweden, Uppsala Imanet, GE Healthcare, Box 967, SE-751 09 Uppsala, Sweden, and ISOF, Consiglio Nazionale delle Ricerche, Via P. Gobetti 101, I-40129 Bologna, Italy

Received February 7, 2007; E-mail: oleksiy.itsenko@biorg.uu.se; chrys@isof.cnr.it

Abstract: Photoinitiated carbonylation of alkyl iodides with [11C]carbon monoxide (11C $t_{1/2}$ = 20.4 min) is enhanced by ketones that have lowest-lying excited triplet state of $n\pi^*$ character. For example, adding 5 mol % of acetophenone increases radiochemical yields from 3 to 59% in brief 6-min long reactions. Similar or higher yields were achieved by adding di-*tert*-butyl peroxide. Since radicaloid $n\pi^*$ exited-state ketones and *tert*-butoxyl radicals have similar reactivity, the photosensitization proceeds most likely via a H-atom transfer mechanism rather than via energy transfer. We propose a mechanism that can account for the enhancement as well as for the formation of observed byproducts. The energy profile obtained by DFT calculations support the feasibility of the mechanism, and observed experimental differences in reactivity could be well rationalized by the calculated data. NBO calculations were performed to further analyze the obtained energetics. Various [*carbonyl*-11C]esters and some [*carbonyl*-11C]amides were synthesized in good radiochemical yields from primary and secondary alkyl iodides illustrating the utility of dialkyl peroxides to accelerate the carbonylations. These findings have potential in elaborating new synthetic protocols for the production of 11C-labeled tracers for positron emission tomography.

Introduction

Positron emission tomography (PET) is a molecular imaging modality that enables assessment of the biochemical function of organs in a living subject using picomolar amounts of tracers appropriately labeled with a positron emitting radionuclide (11C, 15O, 18F, etc). Increasing use of PET in medical diagnostics,[1] life science research, and drug development[2] has motivated the development of the radiochemistry of positron emitters.

Among positron-emitting radionuclides used for the preparation of PET imaging agents (tracers) 11C has a unique position owing to the synthetic diversity of carbon chemistry. In addition, virtually any drug or endogenous substance can be labeled with 11C isotopically, without altering chemical and biochemical properties of the compound. However, the short half-life of 11C ($t_{1/2}$ = 20.4 min) narrows down the selection of reactions useful

for incorporating the radionuclide to fast and, preferably, one-pot procedures.[3] Radiation safeties require that synthetic procedures are highly automated. Hence, the development of fast and reliable methods for the preparation of submicromolar quantities of 11C-labeled tracers is essential to fully exploit versatile applications of PET.

Aliphatic ester functionality R[11C]O2R′ (R = alkyl) has previously been labeled utilizing multistep protocols, using [*carbonyl*-11C]acyl halides[4] or [*carbonyl*-11C]ketenes[5] as the acylating agents, which were obtained from the appropriate Grignard reagents and [11C]carbon dioxide. An alternative route is via [11C]nitriles, starting from hydrogen [11C]cyanide.[6,7] [11C]-Carbon dioxide and hydrogen [11C]cyanide produced using particle accelerators are two of the few chemical forms of 11C

---

(1) *Positron Emission Tomography: Basic Science and Clinical Practice;* Bailey, B. L., Townsend, D. W., Valk, P. E., Maisey, M. N., Eds.; Springer-Verlag: London, 2003.

(2) (a) *PET for Drug Development and Evaluation;* Comar, D., Ed.; Kluwer Academic Publishers: Dordrecht, The Netherlands, 1995. (b) Halldin, C.; Gulyas, B.; Farde, L. *Curr. Pharm. Des.* **2001**, *7*, 1907−1929. (c) Gibson, R. E.; Burns, H. D.; Hamill, T. G.; Eng, W.-S.; Francis, B. E.; Ryan, C. *Curr. Pharm. Des.* **2000**, *6*, 973−989.

(3) Långström, B.; Kihlberg, T.; Bergström, M.; Antoni, G.; Björkman, M.; Forngren, B. H.; Forngren, T.; Hartvig, P.; Markides, K.; Yngve, U.; Ögren, M. *Acta Chem. Scand.* **1999**, *53*, 651−669.

(4) Luthra, S. K.; Pike, V. W.; Brady, F. J. *J. Chem. Soc., Chem. Commun.* **1985**, 1423−1425.

(5) Imahori, Y.; Ido, T. *Med. Chem. Res.* **1995**, *5*, 97−112.

(6) Thorell, J.-O.; Stone-Elander, S.; Elander, N. *J. Labelled Compd. Radiopharm.* **1994**, *34*, 383−390.

(7) Winstead, M. B.; Dougherty, D. A.; Lin, Tz-H.; Khentigan, A.; Lamb, J. F.; Winchell, H. S. *J. Med. Chem.* **1978**, *21*, 215−217.

(8) (a) Kihlberg, T.; Långström, B. Patent WO 2002102711, 2002. (b) Hostetler, E. D.; Burns, H. D. *Nucl. Med. Biol.* **2002**, *29*, 845−848. (c) Miller, P. W.; Long, N. J.; de Mello, A. J.; Vilar, R.; Passchier, J.; Gee, A. *Chem. Commun.* **2006**, 546−548.

Scheme 1. Reaction Mechanism of the One-Pot Procedure Based on the Iodine Atom Transfer Carboxylation (Taken from ref 12)
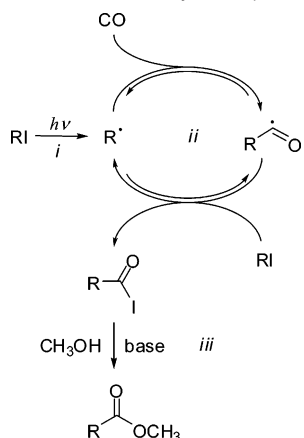
available as starting material for labeling. [^{11}C]Carbon monoxide, which can be prepared by the reduction of [^{11}C]carbon dioxide, has not until recently been much used in labeling because of the difficulties with handling it in microscale. After the development of suitable instrumentation[8] [^{11}C]carbon monoxide has proved to be a useful reagent for labeling,[9] and it was used, in particular, for synthesizing [*carbonyl*-^{11}C]esters via transition metal-mediated carbonylation.[10] This route, though, is limited mainly to compounds in which R is methyl or an aryl moiety, owing to the facility of the competing β-elimination.[11]

Atom transfer radical carbonylation reactions,[12] known also as radical carboxylation and widely applied by Ryu and co-workers, can offer a valuable complement to transition metal carbonylations for the synthesis of aliphatic carboxylic acids, esters, and amides. Scheme 1 illustrates the complex reaction mechanism occurring in a one-pot fashion, which involves (i) radical initiation by photolysis of alkyl iodides, (ii) two reversible steps of chain propagation, and (iii) ionic quenching with the help of a base, to shift the acyl iodide to the desired acyl derivative. To improve the reactions involving primary alkyl iodides, the same group recently introduced a modified protocol in the presence of Pd(0).[13]

The radical carboxylation could have potentiality for widening the range of accessible ^{11}C-labeled compounds. However, experimental conditions for bulk synthesis (e.g., irradiation for

(9) (a) Kihlberg, T.; Långström, B. *J. Org. Chem.* **1999**, *64*, 9201−9205. (b) Audrain, H.; Martarello, L.; Gee, A; Bender, D. *Chem. Commun.* **2004**, 558−559. (c) Doi, H.; Barletta, J.; Suzuki, M.; Noyori, R.; Watanabe, Y.; Långström, B. *Org. Biomol. Chem.* **2004**, *2*, 3063−3066. (d) Rahman, O.; Kihlberg, T.; Långström, B. *Org. Biomol. Chem.* **2004**, *2*, 1621−1626. (e) Karimi, F.; Lånström, B. *Org. Biomol Chem.* **2003**, *3*, 541−546. (f) Rahman, O.; Kihlberg, T.; Långström, B. *J. Org. Chem.* **2003**, *68*, 3558−3562. (g) Karimi, F.; Barletta, J.; Långström, B. *Eur. J. Org. Chem.* **2005**, *11*, 2374−2378. (h) Andersson, Y.; Långström, B. *J. Chem. Soc., Perkin Trans. 1* **1995**, 287−289. (i) Nader, M. W.; Oberdorfer, F. *Appl. Radiat. Isot.* **2002**, *57*, 681−685. (j) Madsen, J.; Merachtsaki, P.; Davoodpour, P.; Bergstrom, M.; Långström, B.; Andersen, K.; Thomsen, C.; Martiny, L.; Knudsen, G. M. *Bioorg. Med. Chem.* **2003**, *11*, 3447−3456.
(10) Kihlberg, T.; Långström, B. *J. Labelled Compd. Radiopharm.* **2001**, *44*, S990−S992.
(11) Crabtree, R. H. *The Organometallic Chemistry of the Transition Metals*, 3rd ed.; Wiley-Interscience: New York, 2000; p 188.
(12) For review, see: Ryu, I. *Chem. Soc. Rev.* **2001**, *30*, 16−25. For the original articles, see: (a) Nagahara, K.; Ryu, I.; Komatsu, M.; Sonoda, N. *J. Am. Chem. Soc.* **1997**, *119*, 5465−5466. (b) Ryu, I.; Nagahara, K.; Kambe, N.; Sonoda, N.; Kreimerman, S.; Komatsu, M. *Chem. Commun.* **1998**, 1953−1954. (c) Kreimerman, S.; Ryu, I.; Minakata, S.; Komatsu, M. *Org. Lett.* **2000**, *2*, 389−391.
(13) Fukuyama, T.; Nishitani, S.; Inouye, T.; Morimoto, K.; Ryu, I. *Org. Lett.* **2006**, *8*, 1383−1386.

several hours and high concentration of carbon monoxide) are not practical at all for the synthesis of radioactive tracers employing short-lived ^{11}C.[14] Nevertheless, modification of the radical-based approach with the use of strong bases (e.g., KOH, BuLi, or LiHMDS) afforded aliphatic [*carbonyl*-^{11}C]esters with good radiochemical yields in short (5−7 min) reaction times.[15] Furthermore, investigating the applicability of photoinitiated radical carbonylation to the synthesis of ^{11}C-labeled compounds it was noticed that reactions employing oxygen nucleophiles produced improved yields when acetone was used as a solvent. Such enhancing effect also became visible when several typical photochemical sensitizers were used in a low quantity (0.05 equiv to the iodide), and it was suggested that they act as energy donors, promoting the photolysis of alkyl iodides.[16]

In this full account we report an important extension of these findings to a general method for the synthesis of aliphatic [*carbonyl*-^{11}C]esters with promising applicability to the preparation of radioactive tracers. To rationalize our findings and place them in a proper context of radical carbonylation mechanism, theoretical calculations of the reaction steps (ii) shown in Scheme 1 have also been performed.

Results and Discussion

Reactions with Carbonyl Triplets. As it is frequently the case, carbonyl triplets react with organic compounds either by energy transfer or by reduction via hydrogen transfer.[17] Eight ketones with different properties were chosen as the photoinitiators of radical carboxylation of 1-iodopentane and methanol using [^{11}C]carbon monoxide (eq 1), to understand their role (Table 1). Four of them have a $n\pi^*$ low-lying triplet state, whereas the other half have a $\pi\pi^*$ character of their triplets. Their triplet energies (E_T) vary in the range 50.4−74.1 kcal mol^{-1}.

$$C_5H_{11}I + [^{11}C]O + CH_3OH \longrightarrow C_5H_{11}[^{11}C]O_2CH_3 \quad (1)$$
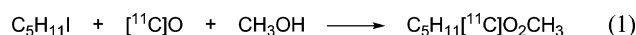
On average, 10−20 nmol of [^{11}C]O mixed with the carrier gas (He, ca. 50 μmol), was used in the syntheses. At first the gas mixture was introduced into a reactor, followed by the solution of 1-iodopentane (0.2 M) and ketone (0.01M) in CH$_3$-OH/THF mixture (1:1, v/v). Then the reactor was pressurized to ca. 38 MPa and irradiated for 6 min at 35 °C using a 200 W Xe lamp equipped with an optical filter, transmitting in the 280−400 nm range. Table 1 shows the conversion of [^{11}C]O and the radiochemical yields of methyl ester in the presence and absence of ketones.

It is clear that the efficiency and effectiveness of the reaction strongly depended on the nature of the excited triplet state of ketone, although the triplet energy might also have played a role. Within the ketones having $n\pi^*$ low-lying triplet states, benzophenone, xanthone, and acetophenone resulted in good conversions and yields, whereas benzil (lower triplet energy) showed the poorest yield. On the other hand, reactions using ketones with $\pi\pi^*$ character of their triplets gave low yields, irrespective of their triplet-state energy.
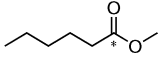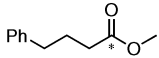
(14) (a) Långström, B.; Bergson, G. *Radiochem. Radioanal. Lett.* **1980**, 43−47. (b) Långström, B.; Öbenius, U.; Sjöberg, S.; Bergson, G. *J. Radioanal. Chem.* **1981**, *64*, 279−286.
(15) Itsenko, O.; Kihlberg, T.; Långström, B. *Eur. J. Org. Chem.* **2005**, 3830−3834.
(16) Itsenko, O.; Långström, B. *Org. Lett.* **2005**, *7*, 4661−4664.
(17) Walling, C.; Gibian, M. J. *J. Am. Chem. Soc.* **1965**, *87*, 3361−3364. Porter, G.; Dogra, S. K.; Loutfy, R. O.; Sugamori, S. E.; Yip, R. W. *J. Chem. Soc., Faraday Trans. 1* **1973**, *69*, 1462−1474.

Table 1. Radiochemical Yield of Methyl [*carbonyl*-^{11}C]Hexanoate from the Photolysis of 1-Iodopentane (0.2 M) with Various Ketones in MeOH/THF (1:1, v/v)

	ketone (0.01 M)	$E_T,^a$ kcal mol^{-1} (triplet state)	conversion [^{11}C]O,^{b} %	purity,^{c} %	yield,^{d} %	N^e
1	acetophenone	74.1 (nπ*)	66 ± 8	89 ± 4	59 ± 9	4
2	benzophenone	69.1 (nπ*)	68 ± 3	82 ± 4	55 ± 4	3
3	xanthone	74.1 (nπ*)	55 ± 7	80 ± 3	44 ± 4	3
4	benzil	54.3 (nπ*)	36 ± 1	70 ± 13	25 ± 5	3
5	*p*-methoxyacetophenone	71.5 ($\pi\pi$*)	15 ± 6	93 ± 3	14 ± 6	3
6	*m*-methoxyacetophenone	72.4 ($\pi\pi$*)	4 ± 2	72 ± 2	3 ± 1	3
7	fluorenone	50.4 ($\pi\pi$*)	3 ± 1	34 ± 23	1 ± 1	3
8	2-acetylnaphthalene	59.5 ($\pi\pi$*)	1	73 ± 8	1	2
9	no ketone		4 ± 1	62 ± 5	3 ± 1	2

^{a} Energy of the lowest triplet excited state; values are taken from ref 18. ^{b} Conversion of carbon monoxide. ^{c} Purity: fraction of the labeled product in crude reaction mixture, determined by HPLC. ^{d} Decay-corrected radiochemical yield calculated as a product (purity) × (conversion of [^{11}C]O). ^{e} Number of runs.
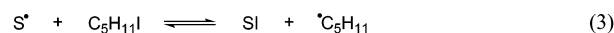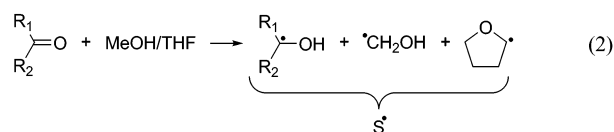
Table 2. Radiochemical Yield of Various [*carbonyl*-^{11}C]Esters from the Photolysis of Iodides (0.2 M) in the Presence of Benzophenone or Acetone

product	conditions	conversion [^{11}C]O,^{a} %	purity,^{b} %	yield,^{c} %	N^f
	MeOH/THF (1:1, v/v), benzophenone (0.01 M)	68 ± 3	82 ± 4	55 ± 4	3
	MeOH/acetone (1:4, v/v)	69 ± 11	76 ± 6	54 ± 4	2
	MeOH/THF (1:1, v/v), benzophenone (0.01 M)	60 ± 2	89 ± 5	53 ± 1	3
	MeOH/acetone (1:4, v/v)	86 ± 1	98 ± 2	85 ± 1	3
	i-PrOH/THF (1:1, v/v), benzophenone (0.01 M)	80 ± 7	75 ± 11	60 ± 14	2
	i-PrOH/acetone (1:1, v/v)	79 ± 5	86 ± 20	69 ± 19	3

*Asterisk indicates the label position. ^{a} Conversion of [^{11}C]carbon monoxide. ^{b} Purity: fraction of the labeled product in crude reaction mixture, determined by HPLC. ^{c} Decay-corrected radiochemical yield calculated as a product (purity) × (conversion of [^{11}C]O). ^{d} Number of runs.

Within the range of the ketones studied, the observed effect is in accordance with hydrogen abstracting abilities of nπ* triplets. Indeed, the triplet of benzophenone, acetophenone, or xanthone abstract hydrogen atoms from the solvent (MeOH/THF) with rate constants in the range 10^5–10^7 M^{-1} s^{-1}, which are significantly greater than that of benzil, fluorenone, or 2-acetonaphtone.[19] In the group of acetophenones (entries 1, 5, and 6) the enhancing effect follows the quantum yields of the photoreduction of these compounds in 2-propanol.[20]

However, the initiation step is not straightforward. The initial hydrogen abstraction from the solvent by the "radicaloid" ketone triplet should be in favor of THF taking into consideration relative rate constants and concentrations (eq 2). All these α-alkoxyl or α-hydroxy-substituted carbon-centered radicals (S•) could react with the alkyl iodide, either by iodine abstraction (eq 3) or by electron transfer following dissociation of radical anion to give the corresponding primary alkyl radical.

$$R_1R_2C{=}O + MeOH/THF \longrightarrow R_1R_2\dot{C}{-}OH + \dot{C}H_2OH + \overset{\cdot}{(THF)} \quad (2)$$

$$S^\bullet$$

$$S^\bullet + C_5H_{11}I \rightleftharpoons SI + \dot{C}_5H_{11} \quad (3)$$

Attempts to carry out the analogous reaction using 0.01 M of acetone as photoinitiator failed (5% conversion of [^{11}C]O and 4% yield). The acetone triplet reacts with MeOH and THF with rate constants only slightly slower than the benzophenone triplet does.[19] However, when acetone was used as solvent, the conversion of [^{11}C]O and radiochemical yield significantly increased. The two first entries of Table 2 show that the

carbonylation of 1-iodopentane using both benzophenone as additive (0.01 M) and acetone as the solvent are comparable. We believe that the excess of acetone is needed to compensate for its low optical absorbance in the window of irradiation, 280–400 nm. We also extended these methods for investigating the substituent effect on the iodide as well as the nature of alcohol. Both 1-iodo-3-phenylpropane and cyclohexyl iodide behave similarly, using methanol or 2-propanol as quenchers, respectively (Table 2).

Reactions with *tert*-Butoxyl Radicals. Following the success of using benzophenone and acetone triplets in the synthesis of various aliphatic [*carbonyl*-^{11}C]esters, we expected that similar or even better results should be brought by photogenerated alkoxyl radicals. It is widely recognized that the reactivity of *tert*-butoxyl radicals is close to that of carbonyl triplets. Comparison of the kinetic data available for the benzophenone triplet with those for the *tert*-butoxyl radicals shows that these two species have a rather similar reactivity toward many substrates.[21]

To optimize the experimental conditions, 0.2 M 1-iodopentane and 0.2 M di-*tert*-butyl peroxide were prepared in CH$_3$OH/THF mixtures, varying methanol molarity, otherwise using the same reaction conditions as described above. Figure 1 shows the dependence of the radiochemical yields of methyl ester on methanol concentration profile. The radiochemical yield was highest when methanol content was about 50%, similar to the

(18) Murov, S.; Carmichael, I.; Hug, G. L. *Handbook of Photochemistry,* 2nd ed.; Marcel Dekker: New York, 1993.
(19) *Handbook of Organic Photochemistry*; Scaiano, J. C., Ed.; CRC Press: Boca Raton, FL, Vol. 2, 1989.
(20) Yang, N.-C.; McClure, D. S.; Murov, S.; Houser, J. J.; Dusenbery, R. *J. Am. Chem. Soc.* **1967**, *89*, 5466–5468.
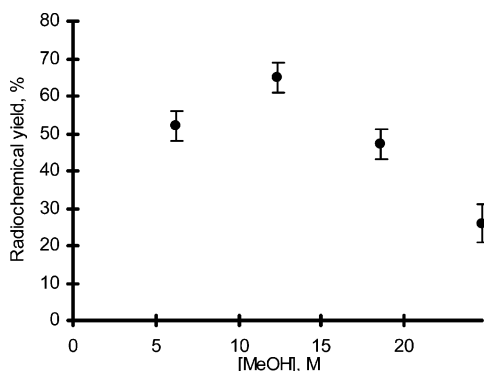
Figure 1. Decay-corrected radiochemical yields of $C_5H_{11}[^{11}C]O_2CH_3$ vs concentration of methanol in the experiments with photogenerated *tert*-butoxyl radical. Error bars represent a standard deviation based on 3–7 experiments. Two values from Figure 1 are also reported in Table 3 (entries 1 and 2).

dependence observed in the ketone-assisted carbonylation (data not shown). With the decrease or increase of methanol content the yield decreased. The lower yields obtained when methanol concentration was high could be an indication of THF participating as a radical mediator in this reaction (eq 3). Indeed, the rate constant of hydrogen abstraction from THF by *tert*-butoxyl radicals is almost 30 times higher than that from methanol.[22]

The replacement of di-*tert*-butyl peroxide (BOOB) by di-cumyl peroxide (COOC), 0.1 M under identical conditions afforded similar results (Table 3, entries 3 and 4), indicating the importance of hydrogen abstraction from the solvent. In the absence of peroxides, radiochemical yields were low (≤5%). It is worth underlining that in all cases a byproduct is formed in 2–6% radiochemical yield, whose retention time matches that of the isotopically unmodified 6-undecanone, that is, the symmetrical ketone (eq 4).[23]

$$RI \quad + \quad [^{11}C]O \quad \longrightarrow \quad \underset{R}{\overset{R}{>}}{=}O \qquad (4)$$
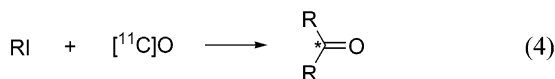
With replacing the starting iodide 1-iodopentane with 1-iodo-3-phenylpropane (Table 3, entry 5) or 3-iodoheptane (Table 3, entry 6), both [^{11}C]O conversion and radiochemical yields remained high, indicating the generality of the method for both primary and secondary alkyl iodides. These reactions also produced small amounts of less-polar byproducts. In the case of entry 5, the byproduct was identified as symmetrical 1,7-diphenylheptan-4[^{11}C]-one based on the retention time of the reference standard. The presence of 1,7-diphenylheptan-4-one was further confirmed by GC–MS (See Supporting Information).

Next, we investigated the presence of alcohol other than methanol in synthesizing several *carbonyl*-^{11}C-labeled esters. Reaction conditions used were as above, that is, 0.2 M alkyl iodide and 0.2 M di-*tert*-butyl peroxide (0.1 mmol each). Alcohols were used in various concentrations, employing THF as the cosolvent. Experimental results are summarized in Table 4. Radio-chromatograms for all reactions contained a notable peak with a retention time matching that of a symmetrical dialkyl ketone (eq 4), where R derives from the alkyl iodide RI used.

With ethanol radiochemical yields were high irrespective of whether ethanol was a singular solvent or reactions were run in EtOH/THF solutions (entries 1 and 2). The formation of symmetrical ketone (eq 4), however, increased considerably with ethanol (13–18% radiochemical yield) compared with analogous experiments with methanol (2–6%). Good radiochemical yields were also obtained with 2-phenylethanol (entry 3). In the synthesis of benzyl [*carbonyl*-^{11}C]valerate and benzyl [*carbonyl*-^{11}C]isovalerate radiochemical yields were low (entries 4 and 5). With benzyl alcohol attempts to improve the synthesis were made (e.g., by doubling the concentrations of the alkyl iodide or performing the reaction in pure benzyl alcohol), but no conditions were found to improve the yield. Using allyl alcohol also resulted in low (≤8%) conversion of [^{11}C]carbon monoxide and unselective formation of numerous labeled byproducts (allyl [*carbonyl*-^{11}C]hexanoate purity was 18–27%).

In reactions using 2-propanol as a nucleophile the conversion of [^{11}C]O was high, but the radiochemical yields of esters are comparable with those of symmetrical ketones (entries 6–8). Furthermore, the comparison of analytical radio-chromatograms for reactions of 1-iodopentane carried out with different alcohols revealed that the yield of the symmetrical ketone increased from 5% in methanol, to 18% in ethanol, to 39% in 2-propanol (cf. Tables 3 and 4)

The method with di-*tert*-butyl peroxide was also useful in the synthesis of amides (Table 5). In the absence of di-*tert*-butyl peroxide there is a notable difference in the reactivity of 1-phenyl-piperazine and 1-adamantylamine (cf. entries 2 and 4, Table 5). The addition of di-*tert*-butyl peroxide allowed obtaining high radiochemical yields with both amines, despite the low (0.1 M) concentration of the nucleophiles.

Reaction Mechanism. The photolysis of di-*tert*-butyl peroxide producing *tert*-butoxyl radicals (eq 5 in Scheme 2) can be regarded as a virtually instantaneous process. Since our 200 W Xe lamp is equipped with an optical filter transmitting in the 280–400 nm range, the light is largely absorbed by RI rather than peroxides below 300 nm (at 280 nm $A_{RI}/A_{BOOB} \approx 9{:}1$ for 0.2 M concentration of each reagent). It is worth underlining that in the absence of dialkyl peroxide the radiochemical yields are below 5%, indicating the important role of *tert*-butoxyl radical as the radical initiator.

The rate constants for the reaction of *tert*-butoxyl radical with methanol, ethanol, 2-propanol, and THF are 2.9×10^5, 1.1×10^6, 1.8×10^6, and 8.3×10^6 M^{-1} s^{-1},[22] respectively, which suggests a reaction of *tert*-butoxyl radical with solvent SH to give α-alkoxy or α-hydroxy substituted carbon-centered radicals (eq 6). These S$^•$ radicals can react with primary or secondary alkyl iodide by iodine abstraction (eq 7).[24]

The concentration of [^{11}C]carbon monoxide in the reaction solution is estimated to be less than 5×10^{-5} to 1×10^{-4} M.[25]

(21) Wagner, P. J. *Acc. Chem. Res.* **1971**, *4*, 168–177.
(22) Paul, H.; Small, R. D., Jr.; Scaiano, J. C. *J. Am. Chem. Soc.* **1978**, *100*, 4520–4527.

(23) The identity of the ketone was substantiated by derivatization: after treating a sample from the crude reaction mixture with an acidified solution of 2,4-dinitrophenylhydrazine the radioactivity peak of the putative ketone in the HPLC-chromatogram disappeared and a new peak at longer retention time emerged. The retention time of the new radioactivity peak exactly corresponds to that of the non-radiolabeled reference compound, the 2,4-dinitrophenylhydrazone of 6-undecanone.
(24) Endothermic halogen atom transfer driven by subsequent ionic reaction has an experimental precedent, see: Curran, D. P.; Ko, S. B. *Tetrahedron Lett.* **1998**, *39*, 6629–6632.

Table 3. Radiochemical Yield of Various [*carbonyl*-^{11}C]Esters from the Photolysis of Iodides (0.2 M) and Dialkyl Peroxides in MeOH/THF (1:1, v/v) or in MeOH

	product	peroxide	[MeOH], M	conversion [^{11}C]O,[a] %	purity,[b] %	yield,[c] %	N[d]
1		BOOB	12	76 ± 3	85 ± 3 (7 ± 2)[e]	65 ± 3 (5 ± 2)[e]	7
2		BOOB	25	29 ± 6	89 ± 1 (5 ± 1)	26 ± 5 (2 ± 1)	4
3		COOC	12	72 ± 7	83 ± 7 (8 ± 4)	59 ± 4 (6 ± 3)	4
4		COOC	25	63 ± 1	81 ± 1 (6 ± 1)	51 ± 1 (4 ± 1)	2
5		BOOB	12	81 ± 1	81 ± 2 (8 ± 1)	65 ± 1 (6 ± 1)	2
6		BOOB	12	70 ± 2	92 ± 2	65 ± 3	3

*Asterisk indicates the label position. [a] Conversion of [^{11}C]carbon monoxide. [b] Purity: fraction of the labeled product in crude reaction mixture, determined by HPLC. [c] Decay-corrected radiochemical yield calculated as a product (purity) × (conversion of [^{11}C]O). [d] Number of runs. [e] Values in parentheses are purity and radiochemical yields for major radiolabeled byproduct (symmetrical ketones).

Table 4. Radiochemical Yield of [*carbonyl*-^{11}C]Esters from the Photolysis of Iodides (0.2 M) and Di-*tert*-butyl Peroxide (0.2 M) in Various ROH or ROH/THF Mixtures

	product	ROH, concentration	conversion [^{11}C]O,[a] %	purity,[b] %	yield,[c] %	N[d]
1		EtOH, 17.1 M	79 ± 1	68 ± 4 (23 ± 4)[e]	53 ± 2 (18 ± 3)[e]	2
2		EtOH, 8 M	61 ± 22	64 ± 3 (23 ± 5)	39 ± 13 (13 ± 5)	3
3		Ph(CH$_2$)$_2$OH, 4 M	46 ± 14	86 ± 4 (1 ± 1)	39 ± 10 (~0.5)	3
4		PhCH$_2$OH, 4 M	10 ± 3	79 ± 1 (~1)	8 ± 3 (~0.1)	3
5		PhCH$_2$OH, 4 M	15 ± 4	69 ± 8 (2 ± 1)	10 ± 2 (~0.3)	3
6		*i*-PrOH, 8 M	81 ± 2	24 ± 9 (31 ± 11)	19 ± 7 (25 ± 10)	3
7		*i*-PrOH, 13 M	78 ± 1	32 ± 5 (49 ± 3)	25 ± 4 (39 ± 3)	2
8		*i*-PrOH, 8 M	81 ± 1	50 ± 4 (40 ± 5)	40 ± 2 (32 ± 3)	2

*Asterisk indicates the label position. [a] Conversion of [^{11}C]carbon monoxide. [b] Purity: fraction of the labeled product in crude reaction mixture, determined by HPLC. [c] Decay-corrected radiochemical yield calculated as a product (purity) × (conversion of [^{11}C]O). [d] Number of runs. [e] Values in parentheses are purity and radiochemical yields for major radiolabeled byproduct (symmetrical ketones).

Table 5. Radiochemical Yield of [*carbonyl*-^{11}C]Amides from the Photolysis of Iodides (0.2 M) and Di-*tert*-butyl Peroxide (0.2 M) Using Amine (0.1 M) in THF as a Solvent
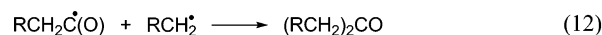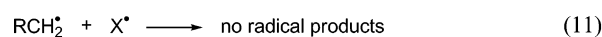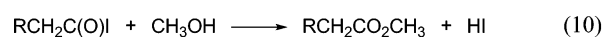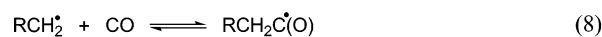
	product	initiator	conversion [^{11}C]O,[a] %	purity,[b] %	yield,[c] %	N[d]
1		BOOB (0.2 M)	72 ± 3	92 ± 2	66 ± 1	3
2		none	trace	–	trace	2
3		BOOB (0.2 M)	80 ± 3	92 ± 4	73 ± 5	2
4		none	72 ± 4	91 ± 3	65 ± 5	3

*Asterisk indicates the label position. [a] Conversion of [^{11}C]carbon monoxide. [b] Purity: fraction of the labeled product in crude reaction mixture, determined by HPLC. [c] Decay-corrected radiochemical yield calculated as a product (purity) × (conversion of [^{11}C]O). [d] Number of runs.

Since the rate constant k_8 for the carbonylation of primary alkyl radicals is 1.7×10^5 M^{-1} s^{-1} and for the reverse reaction k_{-8} is 5.5×10^2 s^{-1},[30] the ratio of equilibrium concentrations in the carbonylation reaction [RCH$_2$C(O)$^{\bullet}$]/[RCH$_2$$^{\bullet}$] is k_8[CO]/k_{-8} ≈ 0.02. Taking into consideration that the steady-state concentration of radicals is expected to be in the range of 10^{-8}–10^{-9} M in our experimental conditions and that radical–radical

termination processes occur at diffusion controlled rates (ca. 10^9 M^{-1} s^{-1}), we suggest that many radicals will terminate by disproportionation and/or combination (eq 11).
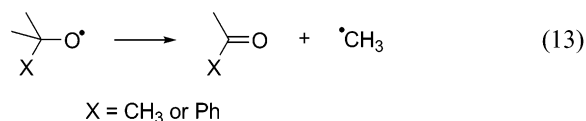
The appearance of unlabeled products from the side reactions is often extremely difficult to notice owing to the low extent of the reaction. However, utilizing the low (radio-)detection limits of [^{11}C]species, the labeled byproducts may be identified. The

Scheme 2. Proposed Reaction Mechanism for the Radical Carboxylation Using [^{11}C]Carbon Monoxide

$$(t\text{-BuO})_2 \xrightarrow{h\nu} 2\ t\text{-BuO}^\bullet \tag{5}$$

$$t\text{-BuO}^\bullet + SH \longrightarrow t\text{-BuOH} + S^\bullet \tag{6}$$

$$S^\bullet + RCH_2I \rightleftharpoons SH + RCH_2^\bullet \tag{7}$$

$$RCH_2^\bullet + CO \rightleftharpoons RCH_2\overset{\bullet}{C}(O) \tag{8}$$

$$RCH_2\overset{\bullet}{C}(O) + RCH_2I \rightleftharpoons RCH_2C(O)I + RCH_2^\bullet \tag{9}$$

$$RCH_2C(O)I + CH_3OH \longrightarrow RCH_2CO_2CH_3 + HI \tag{10}$$

$$RCH_2^\bullet + X^\bullet \longrightarrow \text{no radical products} \tag{11}$$

$$RCH_2\overset{\bullet}{C}(O) + RCH_2^\bullet \longrightarrow (RCH_2)_2CO \tag{12}$$

appearance of symmetrical ketones as byproducts in the syntheses may be attributed to the radical–radical reaction eq 12 under the conditions of ^{11}C-labeling, when the concentration of [^{11}C]carbon monoxide in the solution is low. Incidentally, when we attempted a combined [^{11}C]/(^{13}C) synthesis in a scaled-up reaction employing, besides [^{11}C]O, (^{13}C)O in 1 equiv to RI, the ratio ester/ketone was raised to ca. 15:1, compared with 3:1 in the analogous reaction employing only [^{11}C]O (Table 4, entry 2). This result can be readily explained by the unequal influence of increased carbon monoxide concentration on the individual reaction steps. We can assume that in a given short period of time alkyl radicals are produced at a constant rate by the initiation sequence (eqs 5–7) and the concentration of the reagents is constant. A significant increase (e.g., 100-fold or more) in carbon monoxide concentration will cause a corresponding increase in the ratio [$RCH_2C(O)^\bullet$]/[$RCH_2^\bullet$], governed by equilibrium eq 8. This will result in a minor change or even a decrease in the rate of termination eq 12, but the concentration of the acyl iodide, from which the ester product is formed, will increase linearly with [$RCH_2C(O)^\bullet$]/[$RCH_2^\bullet$] (eq 9).

Interestingly, *tert*-butoxyl radical and cumyloxyl radical are known to decompose unimolecularly with the formation of the methyl radical and the corresponding ketone (eq 13). The rate constants are 2.6×10^4 and 1.4×10^6 s^{-1} (at 30 °C) for *tert*-butoxyl[22] and cumyloxyl radicals,[26] respectively. In the case of *tert*-butoxyl radical the hydrogen abstraction from MeOH is more than 2 orders of magnitude faster then the decomposition, whereas the analogous reaction of cumyloxyl radical is only 5 times faster. Indeed, in the experiment with cumyloxyl radicals in methanol (entry 4 in Table 3) there is a small amount of a

polar labeled product attributable to acetyl ester coming presumably from the $^\bullet CH_3$ radical.

$$\tag{13}$$

$$X = CH_3 \text{ or } Ph$$

The esterification step (eq 10) also needs a further comment. Apparently, for maximizing radiochemical yields, it is necessary to use alcohols in high concentrations, which may be explained by the low nucleophilicity of the alcohols. Indeed, similar reactions with unhindered primary and secondary aliphatic amines or with alkoxide anions usually provided high radiochemical yields when the nucleophiles were used in only 1 equiv to the alkyl iodide, without sensitizers or other additives.[15,27]

In summary, during the 6 min photolysis we consumed sub*milli*molar levels of substrates for the synthesis of sub*mi-cro*molar amounts of [*carbonyl*-^{11}C]esters. This procedure is not considered to be a classical "radical-chain" reaction described by Ryu et al.[12] In our conditions, because [^{11}C]carbon monoxide concentration is low, most of the $RCH_2^\bullet$ radicals roll around and radical–radical reactions compete with radical–molecule reactions to give a variety of products, among which the ketones are detectable because of the presence of the radioactive label in their structure. We term this a "radical-tumble" process.

DFT Calculations. To further investigate the mechanistic proposal outlined above, molecular orbital (MO) calculations with the DFT method were performed on the reactions eqs 7–9 (Scheme 2), using ethanol as the model for the solvent specie involved in the radical mechanism and ethyl iodide as the model alkyl iodide. As mentioned in the previous section, 2-propanol, as well as methanol and ethanol, provide high conversion of [^{11}C]O and reasonable yields of the labeled ester. On the other hand, benzyl and allyl alcohols provide low [^{11}C]O conversion and, consequently, low product yields. To understand these observations better, we included in our study iodine atom transfer from ethyl iodide to the carbon-centered radicals derived from 2-propanol and allyl alcohol.

The geometries, energies, and frequencies of the structures were optimized with the recently described hybrid meta-GGA MPWKCIS1K DFT-functional as detailed in the computational methods section. Table 6 summarizes all iodine atom transfer reactions studied here and the remaining investigated reactions are summarized in Table 7. Initially, DFT calculations were carried out on the reaction of methyl and ethyl radicals with ethyl iodide (eqs 14 and 15) to determine the reaction barriers ($\Delta E^\ddagger$) and energies (ΔE_r). The former equilibrium is chosen because its constant is known to be $K_1 = 23.5$ at 0 °C,[28] (in isooctane solvent) and, therefore, it can be used as a reference for comparison with our calculations in addition to the evaluations discussed in the methods section. The experimental equilibrium constant corresponds to a free energy difference of -1.7 kcal mol^{-1}. As can be seen in Table 6 our calculated reaction energies, -1.4 kcal mol^{-1} (gas phase) and -1.2 kcal mol^{-1} (ethanol), are in good agreement with the experimental value considering that entropy and enthalpy corrections are not included. These corrections are, however, expected to be quite small in this case. Replacing methyl with ethyl radical (eq 15),

(25) Estimated assuming that in a limiting case, under 37 MPa, all gases will dissolve. This value is below the solubility of carbon monoxide under this pressure in, for example, methanol and ethanol, which was calculated using the solubility data from the following: Fogg, P. G. T.; Gerrard, W. *Solubility of gases in Liquids*; Wiley: New York, 1991; pp 274–281.
(26) Baignee, A.; Howard, J. A.; Scaiano, J. C.; Stewart, L. C. *J. Am. Chem. Soc.* **1983**, *105*, 6120–6123.
(27) Itsenko, O.; Kihlberg, T.; Langstrom, B. *J. Org. Chem.* **2004**, *69*, 4356–4360.
(28) Castelhano, A. L.; Griller, D. *J. Am. Chem. Soc.* **1982**, *104*, 3655–3659.
(29) (a) Schiesser, C. H.; Smart, B. A.; Tran, T.-A. *Tetrahedron* **1995**, *51*, 3327–3338. (b) Schiesser, C. H.; Wild, L. M. *J. Org. Chem.* **1998**, *63*, 670–676.
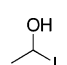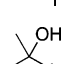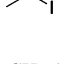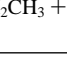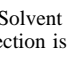(30) Chatgilialoglu, C.; Crich, D.; Komatsu, M.; Ryu, I. *Chem. Rev.* **1999**, *99*, 1991–2069.

Table 6. Reaction Barriers ($\Delta E^{\ddagger}$) and Reaction Energies (ΔE_r) in kcal mol^{-1} for the Reaction of Carbon-Centered Radicals with Ethyl Iodide (CH$_3$CH$_2$I). Mulliken Spin and Charge on the Reacting Carbon Atoms in the Isolated Carbon-Centered Reactant Radicals. All Energies Are Corrected for ZPVE

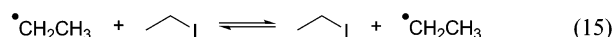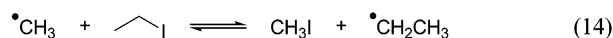|		•CH$_3$	•CH$_2$CH$_3$	⌒OH	⋋OH	⌒O	⤢OH
$\Delta E^{\ddagger}$	SCF	9.0	9.2	8.9	9.9	7.0[a]	22.5
	SCF-PCM	9.3	9.4	9.3	10.1	8.1	21.1
ΔE_r	SCF	−1.4	0.0	2.7	4.6	0.4[b]	19.1
	SCF-PCM	−1.2	0.0	2.8	4.5	1.7	17.3
Spin	SCF	1.10	1.07	0.92	0.90	0.68[c]	0.59[d]
	SCF-PCM	1.10	1.07	0.93	0.92	0.69	0.59
Charge	SCF	−0.28	−0.17	−0.08	0.01	0.03	−0.13
	SCF-PCM	−0.30	−0.20	−0.11	−0.02	0.05	−0.13

[a] At CCSD(T) level, 7.9 kcal mol^{-1}. [b] At CCSD(T) level, 1.9 kcal mol^{-1}. [c] The spin on the oxygen is 0.23. [d] The spin on the terminal carbon is 0.70.

Table 7. Reaction Barriers and Reaction Energies (in kcal mol^{-1}) for the Iodohydrin Dissociation (eqs 17 and 21) and CO Addition (eq 18). All SCF Energies Are Corrected for ZPVE

		SCF		Gibbs	
		gas phase	SCF–PCM	gas phase	solvent
	Iodohydrin Dissociation to Aldehyde or Ketone and HI				
⋋OH/I	TS	22.2	9.5[a]	21.6	10.4[a]
	complex	2.4	6.1[a]	−0.1	6.2[a]
	products	4.7	4.1[a]	−4.9	−3.8[a]
⋋OH/I	TS	19.8	1.8[a]	19.1	2.5[a]
	complex	−2.6	0.5[a]	−5.9	−0.3[a]
	products	0.1	−1.5[a]	−10.6	−10.5[a]
	CO Addition				
•CH$_2$CH$_3$ + CO	TS	6.6	6.3[b]	15.1	13.4[b]
	product	−9.5	−11.6[b]	0.1	−4.0[b]

[a] Solvent correction is based on PCM optimized geometries. [b] Solvent correction is based on gas-phase optimized geometries.

the reaction barrier remains reasonably low ($\Delta E^{\ddagger} = 9.2$ kcal mol^{-1}), suggesting that such an identity reaction may play a role in modulating the radical concentrations, although its contribution in terms of products is nil.

$$•CH_3 + \overset{}{\diagup}I \rightleftharpoons CH_3I + •CH_2CH_3 \quad (14)$$

$$•CH_2CH_3 + \overset{}{\diagdown}I \rightleftharpoons \overset{}{\diagdown}I + •CH_2CH_3 \quad (15)$$

Next we considered the iodine atom transfer from the primary alkyl iodide to the solvent radical. In particular, the equilibrium involving 1-hydroxyethyl radical (eq 16) was investigated. Figure 2 shows that in the transition state for such a transfer, the C−I−C have to be collinear or nearly so ($\Delta E^{\ddagger} = 8.9$ kcal mol^{-1}), whereas the bent transition state is of much higher energy ($\Delta E^{\ddagger} = 25.5$ kcal mol^{-1}). These findings are in line with the linear transition structure reported by Schiesser et al. for iodine transfer between methyl iodide and methyl radical.[29] Therefore, we did not look for bent transition states for any of the other investigated iodine atom transfer reactions. Although the iodine transfer from ethyl iodide to the 1-hydroxyethyl radical is endothermic ($\Delta E_r = 2.7$ kcal mol^{-1}), the reverse reaction is expected to be unimportant under our experimental conditions, because not enough iodohydrin will build-up during the reaction. Indeed, it is expected to dissociate to acetaldehyde
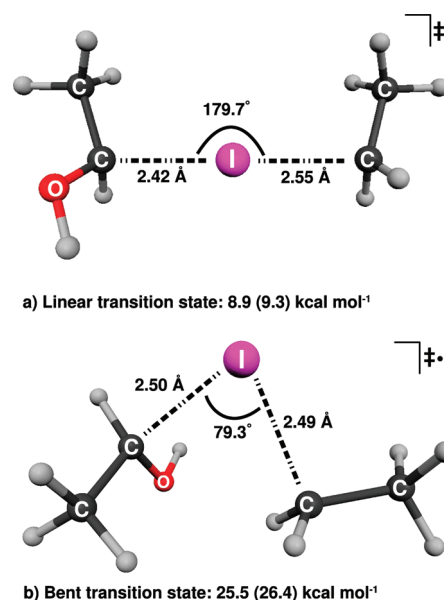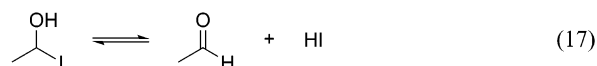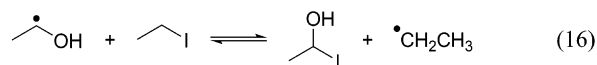
a) Linear transition state: 8.9 (9.3) kcal mol^{-1}

b) Bent transition state: 25.5 (26.4) kcal mol^{-1}

Figure 2. The (a) linear and (b) bent transition state optimized for the reaction: CH$_3$•CH(OH) + CH$_3$CH$_2$I ⇌ CH$_3$CHIOH + •CH$_2$CH$_3$. The energies are relative to the reactants and the PCM corrected energies are given within parentheses.

and hydroiodic acid (eq 17). DFT calculations were also carried out for this reaction.

$$\overset{•}{\diagup}OH + \overset{}{\diagup}I \rightleftharpoons \overset{OH}{\diagdown}I + •CH_2CH_3 \quad (16)$$

$$\overset{OH}{\diagdown}I \rightleftharpoons \overset{O}{\diagdown}H + HI \quad (17)$$

A transition state for the HI elimination on the neutral singlet potential-energy surface was found (Figure 3). An IRC calculation confirmed that the located TS directly leads to the reactant, but following the reaction coordinate in the product direction leads to a hydrogen-bonded post-dissociation complex of the two products with slightly lower electronic energy than the isolated products (Table 7). The elimination of HI is concerted but asynchronous in the sense that breaking of the C−I bond is more progressed than formation of the I−H bond. There is also significant localization of negative charge on the iodine atom (−0.6) and an almost intact O−H bond in the TS (Figure 3a). The significant formation of an isolated iodide in the TS is naturally more pronounced in the polar solvent ethanol, as can
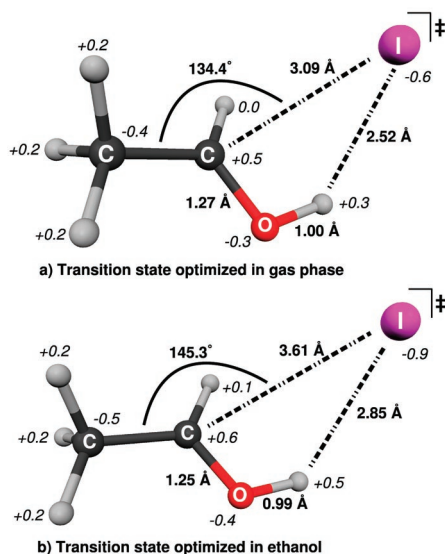
Figure 3. The transition states for HI elimination from CH$_3$CHIOH optimized in (a) gas phase and in (b) ethanol using the PCM model. MK charges are shown with italics style.
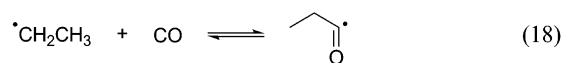
be seen clearly in Figure 3b, which shows the TS optimized using the PCM model of ethanol. Both C−I and I−H distances are longer than in the gas-phase TS, and the charge localized on the iodine atom is higher (−0.9).

The gas-phase barrier for this process, based on zero-point vibrationally corrected electronic energies, is rather high, 22.2 kcal mol^{-1}, and the reaction is endothermic by 2.4 and 4.7 kcal mol^{-1} for formation of the product complex and isolated products, respectively. However, there is a significant entropy contribution to the reaction energy, which is not accounted for in the electronic energies. In the gas-phase we can model the Gibbs free energy of the dissociation process by adding standard thermal corrections based on rigid rotor and harmonic oscillator approximations. Including these corrections, using a temperature of 25 °C, lowers the barrier for dissociation marginally to 21.6 kcal mol^{-1} but the free energy of reaction for formation of isolated products is exothermic by 4.9 kcal mol^{-1}. The product complex is now higher in energy than the isolated products, owing to less favorable entropy. To obtain an estimate of the free energy differences in ethanol solvent, we compute free energies of solvation as the difference between the energy of the optimized gas-phase structure and the energy of the solvated structure that was optimized in solution and apply a thermodynamic cycle using these solvation energies and the gas-phase free energies. Using this procedure, we obtain a barrier for dissociation of 10.4 kcal mol^{-1}, which is significantly lower than the gas-phase barrier, and the free energy of reaction is still slightly exothermic by 3.8 kcal mol^{-1}. It is thus clear that a polar solvent facilitates this step of the proposed sequence of reactions. It is furthermore likely that HI will dissociate in ethanol solution and thus further drive the equilibrium of the iodohydrin dissociation to the right-hand side.
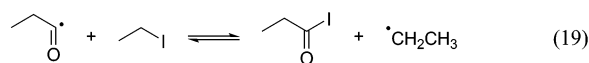
The addition of ethyl radical to carbon monoxide and its reversal are shown in eq 18. Experimental gas-phase Arrhenius activation barriers of 4.8 and 14.6 kcal mol^{-1} are reported for forward and reverse reactions, respectively, and the enthalpy of reaction at 25 °C is reported to be −10.2 kcal mol^{-1}.[30] Our gas-phase calculations gave $\Delta E^{\ddagger} = 6.6$ kcal mol^{-1} and $\Delta H_r = -10.9$ kcal mol^{-1} at 25 °C, which are in good agreement with

the experimental gas-phase data as well as recent computational results.[31] This reaction also involves significant change in entropy, which we include in the description by calculating gas-phase Gibbs free energies, using a temperature of 25 °C. For the free energy of reaction, we obtain a value of 0.1 kcal mol^{-1}, which clearly shows the significant entropy contribution. To estimate the free energy changes for the reaction in ethanol solution, we again make use of a thermodynamic cycle. However, in this case the solvent effects on the gas-phase structures were relatively small, so re-optimization with the solvent model was not performed. We obtain a free energy barrier in ethanol that is 1.7 kcal mol^{-1} lower than the gas-phase barrier, and the reaction is now exothermic by 4.0 kcal mol^{-1}. Hence, polar solvent favors the formation of the acyl radical, and it appears that this step of our proposed reaction sequence is exothermic under our experimental conditions.

Solvent effect on the decarbonylation of acyl radicals has been studied in some details.[30,32] Because of their appreciable dipolar moments, it was suggested that polar solvents stabilize acyl radicals and, therefore, rate constants for decarbonylation decrease and barriers (E_a) increase with higher solvent polarity. Our findings support that the increasing E_a is due to higher solvent stabilization of the acyl radical compared with the transition state and the products of decarbonylation. If we analyze the effect of the solvent on the solute, we find that the transition state is stabilized by only 0.3 kcal mol^{-1} compared with the decarbonylation products, while the acyl radical is stabilized by 2.1 kcal mol^{-1} relative to the products (Table 7, SCF columns).

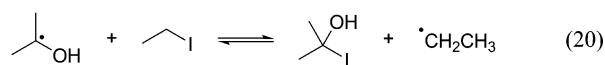$$\cdot CH_2CH_3 \; + \; CO \; \rightleftharpoons \; \text{[acyl radical]} \qquad (18)$$

The next step of our proposed reaction sequence is an iodine transfer from ethyl iodide to acyl radical (eq 19). Like the analogous reaction of 1-hydroxyethyl radical (eq 16), this reaction is computed to be slightly endothermic by 0.4 kcal mol^{-1}. However, the reverse reaction is again expected to be unimportant under our experimental conditions because not enough acyl iodide will build-up during the reaction owing to its consumption by the nucleophile (alcohol or amine). This iodine transfer has a barrier of 7.0 kcal mol^{-1} in gas phase, which is increased to 8.1 kcal mol^{-1} in ethanol solvent. The reaction is also slightly more endothermic in ethanol (1.7 kcal mol^{-1}), so this step in the sequence is somewhat disfavored by polar solvents because of the relative unfavorable solvation of the ethyl radical in such solvents.

$$\text{[acyl radical]} \; + \; \text{[ethyl iodide]} \; \rightleftharpoons \; \text{[acyl iodide]} \; + \; \cdot CH_2CH_3 \qquad (19)$$

To further investigate the effect of the reacting radical on the iodine transfer reaction with ethyl iodide, we calculated the reaction energy and barrier for the reaction with 1-hydroxy-1-methylethyl radical (eq 20).[33] This iodine transfer has a slightly higher barrier than the corresponding reactions with the ethyl radical and the 1-hydroxyethyl radical, 0.7 and 1.0 kcal mol^{-1},

(31) Ryu, I.; Uenoyama, Y.; Matsubara, H. *Bull. Chem. Soc. Jpn.* **2006**, *79*, 1476−1488.
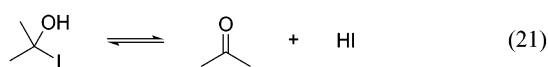(32) (a) Zhang, X.; Nau, W. M. *J. Phys. Org. Chem.* **2000**, *13*, 634−639. (b) Kurnysheva, O. A.; Gritsan, N. P.; Tsentalovich, Y. P. *Phys. Chem. Chem. Phys.* **2001**, *3*, 3677−3682.
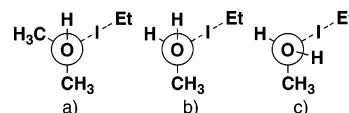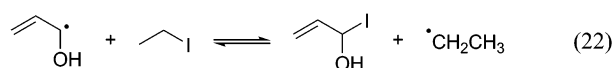
$$\text{(20)}$$

Figure 4. Orientation of the O−H bond in the transition states for iodine atom transfer from ethyl iodide to (a) 1-hydroxy-1-methylethyl radical and (b and c) 1-hydroxyethyl radical.

respectively. This reaction is also more endothermic than the corresponding reaction with the 1-hydroxyethyl radical, 1.9 kcal mol^{-1}, which probably reflects both a slightly higher stability of the reacting 1-hydroxy-1-methylethyl radical and a somewhat lower stability of the sterically more congested product iodide. For the 1-hydroxyethyl radical, the hydroxy hydrogen is staggered between hydrogen and iodine in both the lowest energy transition state and product conformer, whereas for the 1-hydroxy-1-methylethyl radical, the hydroxy hydrogen can only be staggered between methyl and iodine (Figure 4a,b).

The iodine transfer TS for 1-hydroxyethyl radical with the hydroxy hydrogen staggered between methyl and iodine (Figure 4c) has a 0.5 kcal mol^{-1} higher energy than the TS with the hydroxy hydrogen staggered between hydrogen and iodine.

As discussed above, there are reasonably small differences between the carbon-centered radicals derived from 2-propanol and ethanol with respect to the iodine atom transfer step. Hence, to confirm that the theoretical model corresponds well with the experimental observations, we also investigated the elimination of HI from 2-hydroxy-2-iodopropane (eq 21).[34]

$$\text{(21)}$$

These calculations were performed in the manner described above for the HI elimination from 1-hydroxy-1-iodoethane, and all energies are summarized in Table 7. Both gas phase and solvent phase transition structures are overall quite similar to the respective TS shown in Figure 3 for 1-hydroxy-1-iodoethane. However, both the C−I and I−H distances are consistently longer in the 2-hydroxy-2-iodopropane case, and the charge assigned to the iodine atom using the MK scheme is 0.1 more negative in this case. The calculated gas-phase dissociation barriers are slightly lower than for the 1-hydroxy-1-iodoethane case, the free energy barrier is, for example, 19.1 kcal mol^{-1}, which is 2.5 kcal mol^{-1} lower. Furthermore, the gas-phase reaction energies are more favorable in the 2-hydroxy-2-iodopropane case by as much as 5.7 kcal mol^{-1} for the free energy of reaction, which is exothermic by 10.6 kcal mol^{-1} in this case. The most notable difference between the two investigated dissociations is the solvent effect on the reaction barrier, which is significant in both cases. However, in the 2-hydroxy-2-iodopropane case the free energy barrier in solvent is 2.5 kcal mol^{-1}, which is 7.9 kcal mol^{-1} lower than in the 1-hydroxy-1-iodoethane case. Hence, even though the iodine atom transfer step is slightly less favorable when 2-propanol is used, the subsequent dissociation step more than compensates this, and the theoretical model clearly predicts that 2-propanol is at least as efficient as ethanol in terms of forming the alkyl radical and thus giving high conversion of [^{11}C]O, which is in good agreement with our experimental observations.

In experiments with benzyl alcohol and allyl alcohol, we consistently obtained low conversion of [^{11}C]O and low yields. We, therefore, investigated the iodine atom transfer from ethyl iodide to the 1-hydroxy-1-vinylmethyl radical (eq 22). The energies for this reaction are summarized in Table 6.

$$\text{(22)}$$

It is evident that this reaction is the least favorable compared with all the other investigated iodine atom transfer reactions. The solvent effect corrected reaction barrier is 21.1 kcal mol^{-1}, which is 11 kcal mol^{-1} higher than in the equivalent reaction with the 1-hydroxy-1-methylethyl radical. In addition, the reaction is endothermic by 17.3 kcal mol^{-1}. These unfavorable energetics could well rationalize the experimental observations in reactions with benzyl alcohol and allyl alcohol, because there is little reason to expect that the subsequent dissociation step should be more favorable than in the 2-hydroxy-2-iodopropane case described above.

Inspecting the amount of odd spin on the reacting carbon of the isolated radical reactant in the iodide atom transfer reactions (Table 6), we observe that the methyl and ethyl radicals have the highest values ($\sim$1.1), the acyl radical has the second lowest value ($\sim$0.7), whereas the saturated 1-hydroxyalkyl radicals have intermediate values ($\sim$0.9) and the unsaturated 1-hydroxy-1-vinylalkyl radical has the lowest value ($\sim$0.6). It could perhaps be expected that the spin value, as an indication of radical reactivity, would be inversely correlated with the reaction barrier. However, this is not the case for these investigated reactions, as shown in Table 6. In fact, the acyl radical, which has the second lowest spin value, has the lowest reaction barrier, and the 1-hydroxyethyl radical, with an intermediate spin value, has a barrier that is slightly lower (or very similar to) the barrier for methyl and ethyl radicals.

To better understand the calculated iodine atom transfer reaction barriers, we performed natural bond orbital (NBO) analyses for all reactants and transition states (see Supporting Information for details). The most significant feature that differentiates the α-oxygen radicals from the pure alkyl radicals according to the NBO analyses is an oxygen lone pair to C−I (σ*) antibonding orbital hyperconjugation term in the transition states. This hyperconjugation interaction for the transition states with the two types of α-oxygen radicals is illustrated in Figure 5.

The effect of this hyperconjugation is larger for the acyl radical than for the 1-hydroxyalkyl radicals, presumably because of more efficient orbital overlap. For the acyl radical, the donor orbital and the acceptor orbital are in the same plane, owing to the sp^2 hybridization of the carbonyl carbon, whereas for the 1-hydroxyalkyl radicals the donor and acceptor orbitals are somewhat out of plane. In addition, there are no sterical effects for the acyl radical like those discussed above for the 1-hydroxyalkyl radicals. Among the investigated reactant radicals

(33) The electron transfer from (CH$_3$)$_2$COH$^\bullet$ to CH$_3$CH$_2$I is predicted to lead to (CH$_3$)$_2$COH$^+$ + CH$_3$CH$_2$$^\bullet$ + I$^-$, with spontaneous dissociation of the ethyl iodide radical anion. No transition state has been located for this process. The charge-separated products are, as expected, highly unfavorable in the gas phase as revealed by the computed reaction energy (SCF+ZVPE) of 120.4 kcal mol^{-1}. However, when the ethanol environment is included by the PCM model, the reaction becomes more plausible, but is still endothermic with 8.7 kcal mol^{-1}, which is 4.2 kcal mol^{-1} higher than for the iodine atom transfer reaction (see Table 6).
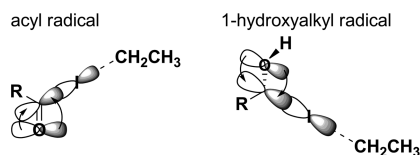
Figure 5. Hyperconjugation in the transition states for iodine atom transfer from ethyl iodide to acyl and 1-hydroxyalkyl radicals.

only the 1-hydroxy-1-vinylmethyl radical contains strongly stabilizing interactions according to the NBO analysis. There is for example a strong C—C π bonding orbital to radical-carbon atom-centered virtual orbital interaction. In addition, there is a strongly stabilizing interaction between a radical-carbon atom-centered occupied orbital and a C—C π^* antibonding orbital. These two interactions correspond well to the two major resonance forms of the radical. The stabilizing interactions in the reactant radical are significantly larger than those found in the TS, which corresponds well with the high barrier found for this reaction.

Conclusion

Both ketones with exited state of nπ^* character and dialkyl peroxides accelerate the photoinitiated radical carbonylation of alkyl iodides with [^{11}C]carbon monoxide using moderately reactive oxygen nucleophiles. On the other hand, ketones with $\pi\pi^*$-type excited-state and hydrocarbon sensitizers do not. The known similarity in the reactivity of alkoxyl radicals and nπ^* triplet-exited-state ketones, which are formed upon photolysis, indicates the common mechanism of their action. These oxygen-centered radicals react with solvent molecules by hydrogen abstraction creating (stabilized) carbon-centered radicals. Solvent-derived radicals are capable of initiating radical sequences by iodine atom transfer from the alkyl iodide. The outcome of the reactions depends on a delicate balance of a complex mechanistic scheme, involving a number of equilibria where the radical termination plays an important role.

Calculated energetics obtained using DFT indicate that the iodine atom transfer step and the subsequent dissociation step are both feasible with barriers no higher than ca. 10 kcal mol^{-1} for the experimentally efficient reactant species, when solvent effects are taken into account. The iodine transfer step is slightly endothermic, but the process is efficiently driven by the subsequent more exothermic dissociation of the iodohydrine. Calculations also rationalize the observed poor yield for allylic and benzylic alcohols, predicting significantly higher barriers for the iodine transfer step.

The applicability of this synthetic methodology for labeling ^{11}C-radiotracers for positron emission tomography (PET) can be envisaged, where attaining good radiochemical yield in a brief reaction, coupled with easy separation of the radioactive compound, are the two important goals to be accomplished. Besides, the results show that high sensitivity of ^{11}C detection may be used in obtaining mechanistic information at a very low extent of the reaction.

Computational Details

The quantum chemical calculations were performed with the Gaussian 03 suit of programs[35] and the abbreviations relating to the employed methods are taken from this program package. Molekel[36] was used for visual inspection of the final geometries and vibrational frequencies, and for making pictures of optimized structures.

The geometries, energies, and frequencies of the structures were optimized with the recently described hybrid meta-GGA MPWKCIS1K DFT-functional,[37,38] using the unrestricted formalism for doublet radicals and the restricted formalism for closed-shell singlets. The geometries were optimized with an ultra-fine integration grid[39] in conjunction with the 6-31+G(d) basis set[40] for the H, C, and O atoms as well as the LanL2DZ basis set[41,42] supplemented with the d-type polarization and p-type diffuse functions of Check et al.[43] for the I atom. The latter basis set is denoted "LanL2DZdp" throughout this work. The nature of all stationary points was characterized by inspection of the vibrational frequencies and normal modes. The single normal mode associated with the imaginary frequency of every transition state was analyzed to verify that it corresponds to the correct distortion of the nuclear framework connecting the reactants with the products. In addition, IRC calculations were performed for the dissociation and addition reactions to further verify that these transition states indeed connect the intended reactants and products. Improved energies at the optimized geometries were calculated with the larger 6-311+G(2df,2p) basis set for the H, C, and O atoms and the LanL2DZdp basis set for the I atom. The inclusion of diffuse functions in DFT calculations was recently recognized as being of general importance for the accuracy of both predicted activation energies and reaction energies.[44] In particular, the 6-311+G(2df,2p) (="MG3S" for H, C, and O atoms in the author's notation)[44] basis set has been shown to yield the best accuracy for both of these quantities comparing a number of different basis sets.[44] Furthermore, the MG3S basis set was for this particular reason chosen in a recent assessment by Truhlar and co-workers of the performance of a large number of DFT functionals for calculating barrier heights of both hydrogen transfer and non-hydrogen transfer reactions.[37]

The MPWKCIS1K/6-31+G(d)/LanL2DZdp method was selected for geometry optimization after an evaluation of the equilibrium geometry of CH$_3$I and the transition structure of the HI + H$^{\bullet}$ $\rightleftarrows$ H$^{\bullet}$ + HI reaction for three hybrid DFT functionals in conjunction with different combinations of basis sets.[45] The computed C—I and C—H bond lengths of CH$_3$I were found to differ by 0.007 and −0.002 Å, respectively, from experimental values obtained by microwave and infrared spectroscopy,[46] while the calculated H—C—I and H—C—H bond angles deviate with

(34) A referee pointed out the possibility that ionic reactions of added solvents with HI, such as the reverse reaction eq 21, ring opening of THF, etc, assist the equilibrium formation of acyl iodide (eq 9) by removing HI produced in the subsequent step (eq 10).[12,24] However, previous results obtained using several amine bases indicate that under our experimental conditions removing HI alone has a minor effect.[15,16]
(35) Frisch, M. J.; et al. *Gaussian 03*, revision C.02; Gaussian, Inc.: Wallingford, CT, 2004.
(36) Flükiger, P.; Lüthi, H. P.; Portmann, S.; Weber, J. *MOLEKEL-4.3*, Swiss Center for Scientific Computing: Manno, Switzerland, 2000.
(37) Zhao, Y.; González-García, N.; Truhlar, D. G. *J. Phys. Chem. A* **2005**, *109*, 2012−2018.
(38) Note that MPWKCIS1K is not a standard keyword of Gaussian 03. The keyword specification for performing calculations in Gaussian 03 at this level is: #MPWKCIS IOp(3/76 = 0590004100).
(39) These criteria are obtained by setting the Int = UltraFine options in Gaussian 03.
(40) Ditchfield, R.; Hehre, W. J.; Pople, J. A. *J. Chem. Phys.* **1971**, *54*, 724−728. (b) Hehre, W. J.; Ditchfield, R.; Pople, J. A. *J. Chem. Phys.* **1972**, *56*, 2257−2261. (c) Hariharan, P. C.; Pople, J. A. *Theor. Chem. Acc. (Theor. Chim. Acta)* **1973**, *28*, 213−222. (c) Hariharan, P. C.; Pople, J. A. *Mol. Phys.* **1974**, *27*, 209−214. (d) Hehre, W. J.; Radom, L.; Schleyer, P. V. R.; Pople, J. A. *Ab Initio Molecular Orbital Theory*; Wiley: New York, 1986.
(41) Wadt, W. R.; Hay, P. J. *J. Chem. Phys.* **1985**, *82*, 284−298.
(42) Hay, P. J.; Wadt, W. R. *J. Chem. Phys.* **1985**, *82*, 299−310.
(43) Check, C. E.; Faust, T. O.; Bailey, J. M.; Wright, B. J.; Gilbert, T. M.; Sunderlin, L. S. *J. Phys. Chem. A* **2001**, *105*, 8111−8116.
(44) Lynch, B. J.; Zhao, Y.; Truhlar, D. G. *J. Phys. Chem. A* **2003**, *107*, 1384−1388.

0.4° and −0.3°, respectively, from the experimental values. The optimized H−I−H transition structure was compared with a quantum chemical prediction[29] computed with the QCISD method in conjunction with Dunning's double-ζ all-electron basis set with an extra set of polarization functions for the H atoms, and the LanL2DZ basis set supplemented with a single set of d-type polarization functions as recommended by Höllwarth and co-workers[47] for the I atom. The MPWKCIS1K/6-31+G(d)/LanL2DZdp computed H−I bond length and H−I−H bond angle of the transition structure deviate 0.001 Å and 3.0° from the corresponding values computed with the QCISD method. The results of these geometry comparisons are very satisfactory, and the MPWKCIS1K functional gave considerably better results than for example the popular B3LYP functional.[45]

The MPWKCIS1K/6-311+G(2df,2p)/LanL2DZdp method was selected for computing energies of the stationary points mainly since Truhlar and co-workers recently found this particular hybrid DFT functional to be one of the three best candidates among a large number of DFT based methods for computing barrier-heights.[37] The MPWKCIS1K functional was even found to outperform QCISD for this purpose. In their assessment, they compared the calculated activation energies against best estimates of classical forward and reverse barrier-heights of 19 hydrogen-transfer reactions and 19 non-hydrogen-transfer reactions given in the HTBH38/04[48] and NHTBH38/04[37] databases, respectively. For all 76 activation energies, the mean-signed-error and the mean-unsigned-error for the MPWKCIS1K/MG3S method were 0.3 and 1.7 kcal mol^{-1}, respectively.[37] Despite the reasonably comparable performances of QCISD and MPWKCIS1K in the assessment by Truhlar and co-workers, we obtain a 6.9 kcal mol^{-1} lower activation energy for the HI + H$^\bullet$ $\rightleftarrows$ H$^\bullet$ + HI iodine atom transfer reaction with MPWKCIS1K/6-311+G(2df,2p)/LanL2DZdp//MPWKCIS1K/6-31+G-(d)/LanL2DZdp than the QCISD prediction reported in ref 29. However, the activation energy obtained with QCISD, using our DFT geometries, is reduced by 4.5 kcal mol^{-1} to 6.8 kcal mol^{-1} when the 6-311+G-(2df,2p)/LanL2DZdp basis set combination is used, which is 2.4 kcal mol^{-1} higher than the DFT result. To further assess the accuracy of the MPWKCIS1K functional for the investigated iodine atom transfer reactions, we also performed CCSD(T) single-point calculations with the 6-311+G(2df,2p)/LanL2DZdp basis set combination on the HI + H$^\bullet$ reaction and with the 6-311+G(d,p)/LanL2DZdp basis set combination for the CH$_3$CH$_2$I + CH$_3$CH$_2$C$^\bullet$(O) $\rightleftarrows$ CH$_3$CH$_2^\bullet$ + CH$_3$CH$_2$C(O)I reaction (eq 19), using the MPWKCIS1K/6-31+G(d)/LanL2DZdp geometries. For the former reaction the CCSD(T) activation energy is 6.1 kcal mol^{-1}, which is 1.7 kcal mol^{-1} higher than the DFT result, and for the latter reaction the CCSD(T) barrier is 8.3 kcal mol^{-1} and the reaction energy is 4.2 kcal mol^{-1}, which is 0.9 and 1.5 kcal mol^{-1}, respectively, higher than the DFT results. Hence, the two high-level ab initio methods (QCISD and CCSD(T)) give similar results, and the MPWKCIS1K functional is within ca. 2 kcal mol^{-1} of these methods for the evaluated reactions.

We have evaluated the bulk solvation effects on the computed relative energies, by performing single-point calculations (MPWKCIS1K/6-311+G(2df,2p)/LanL2DZdp) on the gas-phase geometries using the implicit solvent model, PCM, and the standard parameters for ethanol. These calculations predict in general only a minor influence by the bulk solvent. Large differences were, however, noted when comparing the barrier-heights for the elimination of HI from CH$_3$CHIOH and (CH$_3$)$_2$CIOH in gas-phase and in ethanol. Therefore, we re-optimized the geometries of the species involved in these particular reactions in ethanol at the MPWKCIS1K/6-31+G(d)/LanL2DZdp level using the PCM model.

Atomic charges have been calculated for the gas-phase and PCM ethanol optimized transition structures in the HI elimination reactions by fitting the charges to the electrostatic potential according to the Merz−Singh−Kollman (MK) scheme.[49] Default atomic radii were employed for the O, C, and H atoms (1.4, 1.5 and 1.2 Å, respectively), while 2.5 Å was used for the iodine atom. Two atomic radii for the iodine atom, 2.0 and 2.5 Å, were evaluated for the computation of MK charges. Previously, MK charges for iodine containing molecules have shown to be quite insensitive to the choice of atomic radius of iodine and a value of 2.5 Å has been employed for production purposes.[50] Indeed, the MK charge of the iodine atom changes less than 0.01 in all transition structures, when the iodine radius is enlarged from 2.0 to 2.5 Å.

NBO analysis were carried out to rationalize differences noted for the transition state energies of the iodine atom transfer reactions addressed in the present work. All NBO analyses were performed using the NBO program,[51] which is implemented in the Gaussian 03 suite of programs,[35] at the MPWKCIS1K/6-311+G(2df,2p)/LanL2DZdp level of theory on geometries optimized with MPWKCIS1K/6-31+G(d)/LanL2DZdp. A detailed description of the NBO calculations is provided in the Supporting Information.

Experimental

Materials. [^{11}C]Carbon dioxide was produced with a cyclotron via ^{14}N(p,α)^{11}C nuclear reaction in a gas target containing nitrogen (Nitrogen 6.0) and 0.1% oxygen (Oxygen 4.8). [^{11}C]Carbon monoxide was obtained by the reduction of [^{11}C]carbon dioxide over zink at 400 °C, and handled using an automatic system "Carbon Monoxide Synthia" as described previously.[52] Solvents: THF, methanol, and ethanol were UV spectroscopy grade, acetone was anhydrous grade, and 2-propanol was distilled under nitrogen from sodium borohydride. The following reagents and reference compounds were synthesized using published methods: 4-iodoheptane[53] was synthesized from 2-propylpentanoic acid via a modified[54] Barton decarboxylation; methyl 4-phenylbutanoate[55] and methyl 2-propylpentanoate[56] were synthesized according to ref 57; ethyl 4-phenylbutanoate was synthesized according to ref 58; *iso*-propyl hexanoate[59] was prepared from hexanoyl chloride; and 1-cyclohexanecarbonyl-4-phenylpiperazine[27] was prepared from cyclohexanecarbonyl chloride. The NMR spectral properties for the synthesized compounds were in accordance with published data. All other chemicals were purchased and used as supplied.

Labeling Syntheses Apparatus. The labeling reactions were carried out in a 270-μL stainless steel reactor outfitted with an optical window to allow the irradiation of the reaction mixture by a xenon lamp (280−400 nm). The reactor is a part of the "Carbon Monoxide Synthia", an automated remote-controlled system for handling [^{11}C]carbon monoxide.[52,60]

Analysis of the ^{11}C-Labeled Compounds. The labeled products were routinely identified using known retention times of isotopically

(45) See the Supporting Information for a detailed description of the method evaluation.
(46) Kudchadker, S. A.; Kudchadker, A. P. *J. Phys. Chem. Ref. Data*, **1975**, *2*, 457.
(47) Höllwarth, A.; Böhme, M.; Dapprich, S.; Ehlers, A. W.; Gobbi, A.; Jonas, V.; Köhler, K. F.; Stegmann, R.; Veldkamp, A.; Frenking, G. *Chem. Phys. Lett.* **1993**, *208*, 237−240.
(48) Zhao, Y.; Lynch, B. J.; Truhlar, D. G. *Phys. Chem. Chem. Phys.* **2005**, *7*, 43−52.
(49) Besler, B. H.; Merz, K. M., Jr.; Kollman, P. A. *J. Comput. Chem.* **1990**, *11*, 431−439.
(50) Marynick, D. S. *J. Comput. Chem.* **1988**, *19*, 1456−1469.
(51) Glendening, E. D.; Reed, A. E.; Carpenter, J. E.; Weinhold, F. *NBO, version 3.1.*
(52) Itsenko, O.; Kihlberg, T.; Långström, B. *Nature Protocols* **2006**, *1*, 798−802.
(53) Dostovalova, V. I.; Velichko, F. K.; Fridlina, R. Kh. *Izv. Akad. Nauk SSSR Ser. Khim.* **1987**, 773−778.
(54) Dauben, W. G; Kowalczyk, B. A.; Bridon D. P. *Tetrahedron Lett.* **1989**, *30*, 2461−2464.
(55) Satoh, T.; Unno, H.; Mizu, Y.; Hayashi, Y. *Tetrahedron* **1997**, *53*, 7843−7854.
(56) Madder, A.; Sebastian, S.; Van, Haver, D. V.; De Clercq, P. J.; Maskill, H. *J. Chem. Soc., Perkin Trans. 2* **1997**, *12*, 2787−2793.
(57) Clinton, R. O.; Laskowski, S. C. *J. Am. Chem. Soc.* **1948**, *70*, 3135−3136.
(58) Zelechonok, Yu.; Silverman, R. B. *J. Org. Chem.* **1992**, *57*, 5787−5790.
(59) Travis, B. R.; Sivakumar, M.; Hollist, G. O.; Borhan, B. *Org. Lett.* **2003**, *5*, 1031−1034.

unchanged reference substances, on an HPLC instrument equipped both with UV and radioactivity detectors. The labeled products were purified using semipreparative HPLC. LC−MS was then used to establish molecular masses. For further characterization a combined $^{11}C/^{13}C$ labeling of ethyl 4-phenylbutanoate was performed, using added (^{13}C)-carbon monoxide. The product, ethyl [*carbonyl*-^{11}C]/(*carbonyl*-^{13}C)4-phenylbutanoate, was isolated and, after radioactivity has decayed, analyzed by NMR spectroscopy and GC−MS. The identity of the compound and the labeling position were confirmed by comparing the obtained analytical data of the ^{13}C-substituted product with that of the isotopically unmodified reference compound.

Liquid chromatography analysis was performed using a gradient pump and a variable-wavelength UV detector in series with a β^+ flow detector. LC purification of the labeled products was performed on a remotely controlled HPLC apparatus.[61] Radioactivity was measured in an ion chamber. NMR spectra were recorded at 400 or 500 MHz for ^1H and at 100 or 125 MHz for ^{13}C, at 25 °C. Chemical shifts were referenced to the solvent signal in ^{13}C spectra (77 ppm) and the residual solvent proton signal in ^1H spectra (7.26 ppm). LC−MS analysis was performed using electrospray ionization in the ESI+.

Synthesis of Methyl [*carbonyl*-^{11}C]Hexanoate in the Presence of Various Sensitizers. A sensitizer (0.005 mmol) was placed in a crimp-top capped vial (1 mL, flushed beforehand with nitrogen to remove air) and dissolved in THF (250 μL). Then methanol (250 μL) and iodopentane (0.1 mmol) were added to the solution. The resulting solution was pressurized (∼38 MPa) in the reactor already containing [^{11}C]carbon monoxide ($10^{-8}-10^{-9}$ mol) in helium. The mixture was irradiated with a xenon lamp (280−400 nm) at 35 °C with stirring for 6 min and then transferred from the reactor to a capped vial, held under reduced pressure. After the radioactivity in the vial was measured, the vial was purged with nitrogen (to remove unreacted [^{11}C]O) and the remaining radioactivity was measured again to determine the fraction of [^{11}C]carbon monoxide that reacted (conversion of [^{11}C]O). A sample from the reaction mixture was analyzed by HPLC to determine the purity of the labeled product and radiochemical yield.

Synthesis of Methyl [*carbonyl*-^{11}C]Esters Using Di-*tert*-butyl Peroxide. An alkyl iodide (0.1 mmol) was placed in a crimp top capped vial (1 mL, flushed beforehand with nitrogen to remove air) and dissolved in THF. Then an alcohol and di-*tert*-butyl peroxide (0.1 mmol) were added to the solution. The concentration of alcohol in THF is denoted in Table 3 and Table 4; some of the reactions were run in pure alcohols. The resulting solution was pressurized (∼38 MPa) in the reactor already containing [^{11}C]carbon monoxide ($10^{-8}-10^{-9}$ mol) in helium. The mixture was irradiated with a xenon lamp (280−400 nm) at 35 °C with stirring for 6 min and then transferred from the reactor to a capped vial, held under reduced pressure. After the radioactivity in the vial was measured, the vial was purged with nitrogen (to remove unreacted [^{11}C]O) and the remaining radioactivity was measured again to determine the fraction of [^{11}C]carbon monoxide that reacted. A sample from the reaction mixture was analyzed by HPLC to determine the purity of the labeled product and radiochemical yield. The reaction mixture was diluted with an aceto-nitrile−water mixture (0.6 mL) and injected on the semipreparative LC for purification.

Synthesis of Methyl [*carbonyl*-^{11}C]Hexanoate Using Dicumyl Peroxide. Dicumyl peroxide (0.05 mmol) was placed in a crimp-top

vial (1 mL, flushed beforehand with nitrogen to remove air) and dissolved in THF (250 μL). Then methanol (250 μL) was added to the solution, and then iodopentane (0.1 mmol) was added. The resulting solution was pressurized (∼38 MPa) in the reactor already containing [^{11}C]carbon monoxide ($10^{-8}-10^{-9}$ mol) in helium. The mixture was irradiated with a xenon lamp (280−400 nm) at 35 °C with stirring for 6 min and then transferred from the reactor to a capped vial, held under reduced pressure. After the radioactivity in the vial was measured, the vial was purged with nitrogen (to remove unreacted [^{11}C]O) and the remaining radioactivity was measured again to determine the fraction of [^{11}C]carbon monoxide that reacted. A sample from the reaction mixture was analyzed by HPLC to determine the purity of the labeled product and radiochemical yield.

[*carbonyl*-^{11}C]Amides were synthesized in a similar manner as [*carbonyl*-^{11}C]esters using di-*tert*-butyl peroxide and amines (0.05 mmol).

Ethyl [*carbonyl*-^{11}C]/(*carbonyl*-^{13}C)4-Phenylbutanoate. A capped LC vial (1 mL volume) was flushed with nitrogen to remove air. 1-Iodo-3-phenylpropane (16 μL, 0.1 mmol) was placed into the vial followed by ethanol (250 μL) and acetone (250 μL). The reactor was filled first with [^{11}C]carbon monoxide ($10^{-8}-10^{-9}$ mol) in helium and then with (^{13}C)carbon monoxide (approximately 0.1 mmol). After that, the solution of the iodide and alcohol was transferred to the reactor, the reaction mixture was pressurized to ∼38 MPa and irradiated (xenon lamp, 280−400 nm) for 1 h with stirring. During this time the temperature of the reactor grew from 35 to 55 °C. The crude reaction mixture was then transferred from the reactor to a capped vial, held under reduced pressure. The crude product was diluted with acetonitrile (0.6 mL) and purified by the semipreparative LC. ^1H NMR (500 MHz, CDCl$_3$, 25 °C): δ 7.31−7.26 (m, 2H), 7.22−7.16 (m, 3H), 4.12 (dt, $J_{H,C}$ = 3.1 Hz, 2H), 2.65 (m, 2H), 2.32 (m, $J_{H,C}$ = 7.3 Hz, 2H), 1.96 (m, $J_{H,C}$ = 4.3 Hz, 2H), 1.25 (t, 3H). ^{13}C NMR (125 MHz, CDCl$_3$, 25 °C): δ 173.5 (strongest), 141.4, 128.48, 128.36, 125.9, 60.3 (d, $J_{C,C}$ = 2.6 Hz), 35.1 (d, $J_{C,C}$ = 3.8 Hz), 33.7 (d, $J_{C,C}$ = 57.3 Hz), 26.5 (d, J_{CC} = 1.5 Hz), 14.2 (d, J_{CC} = 2.2 Hz).

Supporting Information Available: Computational data: total SCF energies for all stationary structures; zero-point vibrational energies (ZPVE) for all stationary structures; thermal contribution to Gibbs free energy at 298.15 K and 1.0 atm, and total PCM Free energy in solution for selected structures; *xyz*-matrices for the stationary structures involved in the iodine atom transfer reactions, with imaginary frequencies for the transition structures; evaluation of DFT methods for optimizing geometries of stationary points; natural bond orbital analysis; references including complete ref 35; Gaussian archives for all the investigated stationary points. Experimental data: the molar absorptivity of iodopentane, di-*tert*-butyl peroxide, and dicumyl peroxide between 280 and 400 nm; ^1H and ^{13}C spectra of ethyl (*carbonyl*-^{13}C)4-phenylbutanoate; EI-MS spectra of ethyl 4-phenylbutanoate, ethyl (*carbonyl*-^{13}C)4-phenylbutanoate, and 1,7-diphenylheptan-4-one. This material is available free of charge via the Internet at http://pubs.acs.org.

JA0707714

(60) The experimental setup is described in the following: Långström, B.; Kihlberg, T.; Itsenko, O. Patent WO2006064349, 2006.

(61) Bjurling, P.; Reineck, R.; Westerberg, G.; Gee, A. D.; Sutcliffe, J.; Långström, B. In *Proceedings of the VIth workshop on targetry and target chemistry*; TRIUMF: Vancouver, Canada, 1995; pp 282−284.